




Improving Efficiency Through the Publication of Expected Distances for Standard Terminal Arrival Routes

Jan Krummen ^{*,1} Timothé Krauth ¹, Jan Allendorf,² and Raphael Monstein ^{1,3}

¹Centre for Aviation, Zurich University of Applied Sciences, Winterthur, Switzerland

²Swiss International Air Lines, Kloten, Switzerland

³SkAI Data Services, Zurich, Switzerland

*Corresponding author: jan.krummen@zhaw.ch

(Received: 19 November 2024; Revised: 30 January 2025; Accepted: 30 January 2025; Published: 17 February 2025)

(Editor: Xavier Olive; Reviewers: Tatiana Polishchuk and Junzi Sun)

Abstract

Accurate pre-flight fuel planning is essential to ensure that an aircraft carries enough fuel for a safe flight, while avoiding unnecessary weight that reduces efficiency. However, at certain airports, frequent short-cuts on arrival can lead to systematic discrepancies between the nominal STAR (Standard Terminal Arrival Route) distances used for fuel planning and the actual distances flown. This, in turn, can result in aircraft carrying unnecessary excess fuel. To address this issue, some airports have begun to publish expected STAR distances for specific procedures in the Aeronautical Information Publication, allowing operators to plan fuel more accurately. This paper examines the impact of providing expected STAR distances by analysing one year of ADS-B data from Geneva, Munich and Rome Fiumicino airports. The study compares the observed distances flown with the full and expected STAR distances and presents econometric models to identify factors influencing the actual flown distances. In addition, fuel calculations are presented to estimate the potential benefits of publishing expected distances at airports that do not currently provide this information. The results show that for most of the STARs analysed, significant differences between observed flight distances and full STAR distances exist. However, these discrepancies are mitigated by the availability of published expected distances at Munich and Rome. The econometric model highlights consistent influencing factors such as STAR shape, shortcut potential, peak traffic hours, and weather conditions, although some effects are more location-specific. The fuel savings analysis suggests that adopting this practice at more airports could significantly reduce unnecessary fuel burn and associated emissions. Overall, this paper increases the understanding of how publishing expected STAR distances can improve fuel planning accuracy, operational efficiency, and environmental sustainability.

Keywords: Standard Terminal Arrival Route; Aeronautical Information Publication; Route Shortcut; Horizontal Flight Efficiency; Fuel Savings

1. Introduction

Before each flight, pilots must determine the amount of fuel required for the planned trip. This pre-flight fuel planning is crucial to ensure there is sufficient fuel for a safe journey, while also minimizing excess weight to reduce fuel consumption. This fuel calculation is broken down into several components, each addressing a specific aspect of the flight. For example, taxi fuel accounts for the fuel required from engine start to take-off, while trip fuel accounts for the fuel required for the actual flight from take-off to landing at the destination. Additional fractions, called contingency

fuel and alternate fuel, are included to account for eventualities such as adverse weather, re-routing, or diversion to an alternate airport. [1].

Trip fuel is typically the largest portion of the total fuel required for a flight and includes the estimated fuel for the en-route segment as well as the departure and arrival phases. Therefore, fuel consumption for the Standard Instrument Departure (SID) and the Standard Terminal Arrival Route (STAR) is also accounted for in this part. SID and STAR refer to pre-defined air traffic service routes that are essential for streamlining Instrument Flight Rule (IFR) traffic into and out of airports. SIDs guide aircraft from the runway to en-route airspace during departures, while STARs guide aircraft from en-route airspace to a specified fix or navigational aid, allowing a smooth transition to an approach. [2]

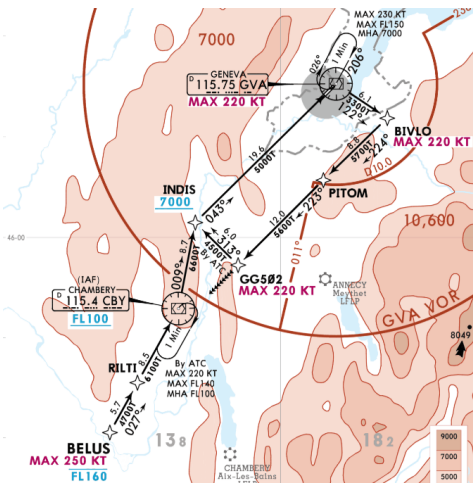
During pre-flight planning, crews cannot predict with certainty which specific SID and STAR will be used, resulting in some uncertainty regarding the required fuel demand for a flight. ICAO Document 9976 [3], which contains guidance material on flight planning and fuel management, therefore advises operators to calculate trip fuel based on lengthy IFR departure and arrival routes, such as the longest SID and STAR, introducing a degree of conservatism. Operators who are able to estimate the likelihood of specific SID/STAR combinations for a given city pair may, however, choose to plan fuel using these expected procedures and account for potential additional distance that could be flown, e.g. in the contingency fuel, thereby reducing unnecessary conservatism and more accurately reflecting actual track miles flown.

Using the full distance of the expected STAR for fuel planning can sometimes be overly conservative. This is the case when air traffic control frequently clears aircraft for more direct approaches, bypassing large sections of the full STAR. Such shortcuts can significantly reduce the actual distance flown, thereby improving horizontal flight efficiency. However, this, in turn, leads to aircraft carrying excess fuel for procedures that are not fully flown.

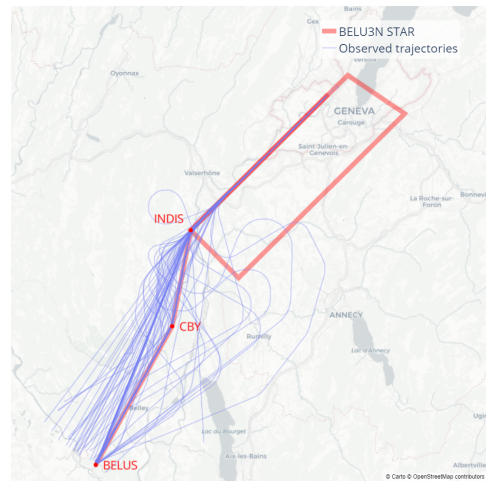
An example of a STAR, where the actual distance flown is usually significantly shorter than the published route, is the *BELUS 3N* STAR at Geneva Airport. As shown in Figure 1a, the published procedure requires aircraft to fly an upwind leg at a higher altitude along the approach path to runway 04, overfly the airport, then turn right to fly a 20 NM downwind leg before turning base for the final approach. If flown as published, the total distance from the STAR's initial waypoint to the runway threshold is approximately 93 NM. In practice, however, most aircraft are cleared for a straight-in approach after passing waypoint *BELUS*, as shown in Figure 1b. The median distance flown for all *BELUS 3N* approaches in the year 2023 was approximately 40 NM, meaning that flights planned considering the entire procedure carry excess fuel for over 50 NM of the arrival that is never used.

To address this, some Air Navigation Service Providers (ANSPs), such as DFS and ENAV, publish expected flight distances for different STAR procedures at specific airports in the Aeronautical Information Publication (AIP), allowing operators to use these expected rather than full STAR distances for flight and fuel planning purposes. The way in which expected distances are published may vary from country to country. For example, the German ANSP *DFS* provides expected STAR distances valid throughout the day for Munich Airport, with any deviation from these distances treated as a delay [4]. In contrast, the Italian counterpart *ENARE* requires the planning of the full STAR distance for flights landing at Rome Fiumicino Airport during defined peak periods, but provides reduced distances for off-peak periods [5].

To the authors' knowledge, no published research has directly addressed the specific topic of publishing expected STAR distances to optimize trip fuel calculations. This paper attempts to fill this gap by conducting a series of analyses. First, historical data from Geneva, Munich, and Rome are examined to gain insight into how approaches at these airports are flown in practice. The analysis



(a) Published *BELUS 3N STAR* for southwest arrivals to runway 04 at Geneva Airport. Copyright © 2023 Navigraph / Jeppesen



(b) Random sample of 100 ADS-B trajectories from 2023 utilising the *BELUS 3N STAR* at Geneva Airport.

Figure 1. Comparison between the published *BELUS 3N STAR* and actual flight trajectories flown along this arrival route.

compares the distribution of flown distances with the full STAR distance for all three airports and, for Munich and Rome, with the published expected distances. In the second part of the analysis, the focus shifts to trying to identify external factors that affect the actual STAR distances flown, again using data from the same three airports. Finally, the paper also aims to quantify the potential fuel savings that could be achieved by publishing expected distances for the specific case of the *BELUS 3N* procedure at Geneva Airport, and to highlight the wider potential for similar measures at other airports.

The remainder of this paper is structured as follows: Section 2 presents the steps taken to generate the data required for the study. Section 3 presents the analysis of published versus flown STAR distances, comparing actual flight data with full and expected distances at Geneva, Munich, and Rome Airports. The following Section 4 provides insights into the identification of external factors influencing the flown STAR distances at the three airports. Additionally, Section 5 presents the quantification of the potential fuel savings that could be achieved by publishing expected distances for the *BELUS 3N* approach at Geneva Airport. Finally, Section 6 discusses the wider implications of the findings of this thesis, leading to the conclusion in Section 7.

2. Data Procurement and Preprocessing

ADS-B data for the full year 2023 were sourced from the OpenSky Network [6] for the three airports under consideration: Geneva (LSGG), Munich (EDMM), and Rome Fiumicino (LIRF). The data was retrieved using geographical boundaries tailored to each airport, with sizes adjusted to ensure complete coverage of the full extent of all STARs. These boundaries vary according to the extent of the STARs at each location and correspond to sizes ranging from approximately 130x130 NM to 180x180 NM. Several processing steps were applied to the trajectory data for each location using the *Traffic* Python library [7]. These include applying standard filtering, reducing the data to landings at the designated airport, removing go-arounds, and enhancing the data by adding runway information as well as a unique flight identifier for each trajectory.

For each airport, a subset of four STARs was selected for analysis, prioritising those with the greatest potential for shortcuts. These were identified by large differences between the nominal STAR route

distance and the direct distance between its first and last waypoints. Additionally, for Munich and Rome, only STARs with expected distances provided in the respective AIP were considered. The STARs selected on the basis of the specified criteria are *AKITO 3R*, *BELUS 3N*, *KINES 2N* and *LUSAR 2N* for Geneva (LSGG); *BETOS 1A*, *LANDU 1B*, *NAPSA 1B* and *ROKIL 1A* for Munich (EDDM); as well as *ELKAP 2A*, *LAT 2C*, *RITEB 2A* and *VALMA 2C* for Rome Fiumicino (LIRF). Figure 2 provides a visual representation of the selected STARs at each airport.

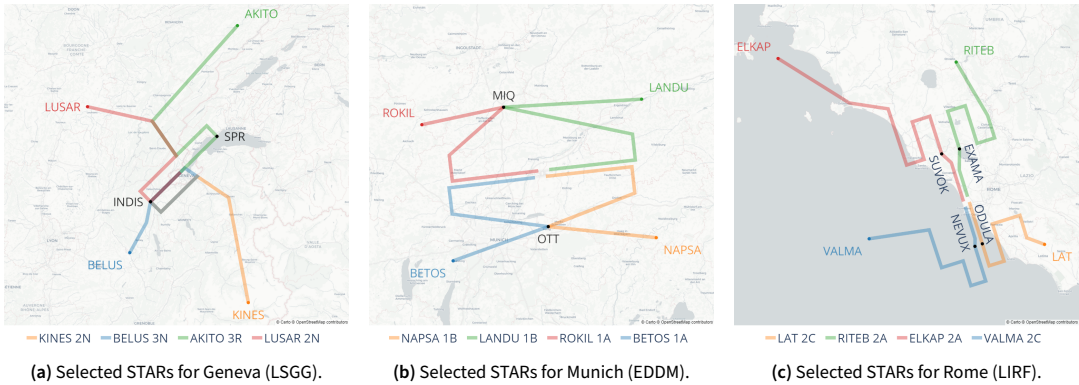
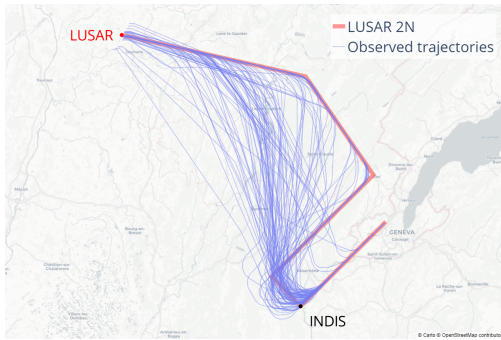


Figure 2. Visualisation of the selected STARs at each airport. The routes plotted include both the STARs and the subsequent approach to the runway threshold. The black waypoints indicate the STAR endpoints. In the case of Munich and Rome, each STAR serves both parallel runways, but only one approach per STAR is shown for clarity.

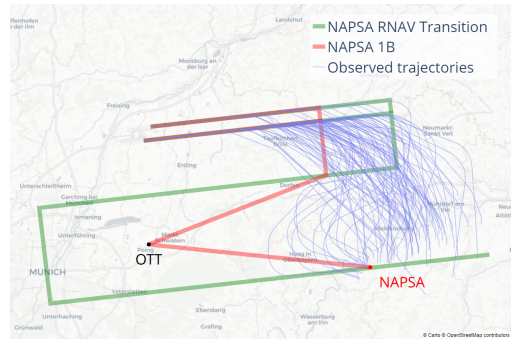
Next, it was necessary to filter the trajectory data for each airport to retain only flights that approached the airport using one of the selected STAR procedures, and to add the information about which STAR was used to the data. This filtering was again done using functions provided by the *Traffic* library, with slightly different approaches depending on the airport. In Geneva, each STAR is uniquely associated with a specific initial waypoint and landing runway. Flights following a particular STAR were easily identified as those passing its initial waypoint and landing on the corresponding runway. In Rome, several STARs share the same initial waypoint and serve the same runways. For the data at this airport, the identification process has, therefore, been adapted to include the additional condition of passing the final waypoint of the STAR, to ensure the correct identification of trajectories following one of the STARs of interest. At Munich Airport, each selected STAR has a corresponding RNAV transition that shares the initial waypoint and serves the same runways. However, as shown by the *NAPSA* approaches in Figure 3b, most flights appear to be vectored to the approach and never really align with either procedure, making it almost impossible to distinguish between the two even when additional constraints are added. Consequently, the same classification method was used as for Geneva, relying solely on the combination of the initial waypoint and the runway. It should be noted, however, that this technique is likely to include flights following RNAV transitions in the data.

All remaining trajectories were then cropped based on the available STAR and runway information, retaining only the portion between passing the initial STAR waypoint and the moment the aircraft crossed the runway threshold. Figure 3 shows examples of trajectories for two different STARs at Geneva and Munich Airports, cropped using this method. Finally, the cumulative distance travelled was determined for each trajectory and added to the data as an additional column.

Based on the resulting processed trajectory data, a dataframe was generated for each airport, summarising key information about each flight to facilitate subsequent analyses. Table 1 details the columns in these data frames.



(a) Visualization of 100 randomly selected trajectories classified as following the LUSAR 2N STAR at Geneva Airport.



(b) Visualisation of 100 trajectories classified as following the NAPSAs 1B STAR at Munich Airport.

Figure 3. Classified and cropped trajectories along with the nominal route for two different STARs at Geneva and Munich Airport.

Table 1. Overview of the tables generated for all three airports, containing key information used in subsequent analyses.

Column	Description
ID	A unique identifier linking the row to the corresponding trajectory data
Typecode	The ICAO type code of the aircraft
Start	Timestamp when the aircraft passes the first waypoint of the STAR
Stop	Timestamp when the aircraft crosses the runway threshold
Runway	Designator of the landing runway
STAR	Name of the STAR procedure used by the aircraft
Distance	Total distance traveled by the aircraft from the initial waypoint of the STAR to the runway threshold

3. Analysis of Flown STAR Distances

This section provides an analysis of how the selected STARs at the three airports are flown in practice, and compares the observed distances with the published distances of the full STAR procedures. For Munich and Rome, this comparison is extended to the expected distances published in the AIP described in Figures 4 and 5.

4. Flugplanung

Im Gegensatz zum Flugplan können nachfolgende Entfernungen vom Anfangspunkt der STAR bis zur Landung als zu erwartende Flugentfernung für die Flug- und Treibstoffplanung angenommen werden. Abweichungen davon können als Verzögerung betrachtet werden.

4. Flight planning

In contrast to the flight plan, the following distances from the starting point of the STAR to the landing may be regarded as the expected flight distance for flight and fuel planning purposes. Any deviations from this may be regarded as a delay situation.

STAR Bezeichnung/ STAR ID	Betriebspiste/ RWY in use	Durchschnittliche Flugentfernung/ Average flight distance (NM)
BETOS1A	08L/08R	53
BETOS1B	26L/26R	68
LANDU1A	08L/08R	66
LANDU1B	26L/26R	44
NAPSA4A	08L/08R	69
NAPSA1B	26L/26R	47
ROKIL1A	08L/08R	43
ROKIL1B	26L/26R	72

Figure 4. Extract displaying the expected STAR distances at Munich Airport, as published in the DFS AIP for flight planning purposes. Adapted from [4].

To analyze the difference between actual flown distances and expected flight distances, we visualize the distribution of observed approach distances alongside reference lines indicating both the full STAR distances and, where applicable, the expected STAR distances. Since Rome distinguishes between expected flight distances during peak and off-peak periods, we further compare the distribution of flight distances for each STAR conditionally on these time frames. Rush periods for

2.1.1 Fuel Planning and Management

During peak hours (table 1), the expected flight distance corresponds to the nominal length of the P-RNAV, as published in AIP-Italia AD2 LIRF.

Table 1	
RUSH HOUR (Local Time)	
0630 - 0900	
1100 - 1400	
1630 - 1800	
1900 - 2100	
Remark:	
summertime LT=UTC+2h	
wintertime LT=UTC+1h	

Outside the aforementioned peak hours, the nominal distances of each P-RNAV can be reduced (expected flight distance) according to the indications contained in the following tables (tab. 2 - tab.3):

Table 2				
STAR 16				
	STAR TO IAF	RUSH HOUR	OUT OF RUSH	SAVED MILES
ELKAP 2A	ELKAP - SUVOK	112.9	92.9	20
XIBIL 2A	XIBIL - SUVOK	102.9	82.9	20
GILIO 2A	GILIO - SUVOK	96.1	76.1	20
VALMA 2A	VALMA - SUVOK	87.5	67.5	20
ESINO 2A	ESINO - SUVOK	85.4	65.4	20
RITEB 2A	RITEB - EXAMA	76	56	20
LAT 2A	LAT - EXAMA	84	64	20
MOPUV 2A	MOPUV - EXAMA	96.6	76.6	20

Table 3				
STAR 34				
	STAR TO IAF	RUSH HOUR	OUT OF RUSH	SAVED MILES
ELKAP 2C	ELKAP - ODULA	139.8	124.8	15
XIBIL 2C	XIBIL - SUVOK	129.8	114.8	15
RITEB 2C	RITEB - ODULA	96	81	15
GILIO 2C	GILIO - ODULA	123	108	15
LAT 2C	LAT - ODULA	57.3	37.3	20
MOPUV 2C	MOPUV - ODULA	93.9	73.9	20
VALMA 2C	VALMA - NEVUX	77	62	15
ESINO 2C	ESINO - NEVUX	50	35	15

Figure 5. Extract displaying the expected STAR distances at Rome Fiumicino Airport, with separate values for on-peak and off-peak periods, as published in the ENAV AIP for flight planning purposes. Adapted from [5].

3.1 Geneva

Figure 6 shows the distribution of observed distances for the selected arrivals at Geneva airport. The observed patterns can be grouped into two pairs with similar characteristics. For *KINE2N* and *LUSA2N*, the full STAR distance lies within the distribution of observed distances, but towards the upper tail with the majority of observations below. They also both show a similar offset between the median observed distances and the full STAR distance, which is about 13 NM shorter for *KINE2N* and about 17 NM shorter for *LUSA2N*. In contrast, the plots for *BELU3N* and *AKIT3R* show the majority of the distribution of observed distances well below the full STAR distance, with only a few outliers reaching distances similar to the full STAR distance. The gap between the median observed distances and the full STAR distance is also much larger, with the median observed distance being 45 NM shorter for *AKIT3R* and 53 NM shorter for *BELU3N*.

A look at Figure 7, which shows the distributions distinguishing between rush and out-of-rush periods, confirms the same overall picture. It further reveals that flights landing during off-peak periods are, on average, flying shorter distances than during peak periods for all four approaches examined, although the magnitude of the effect varies slightly for the four STARs.

3.2 Munich

In contrast to Geneva, Figure 8 depicts a fairly consistent picture in the overall distributions for all four approaches analysed at Munich airport. For each STAR, the distribution of observed distances is well below the full STAR distance, with the median of the distribution located between 24 and 46 NM below the full STAR distance, depending on the approach. As mentioned above, Munich has expected STAR distances published in the AIP, represented by the green horizontal lines in the plots. The expected distances are consistently positioned near the upper end of the distribution, meaning that they are closer to the main part of the distribution while most of the observed distances still fall below this threshold. Specifically, the expected distance is consistent with the 95th percentile of

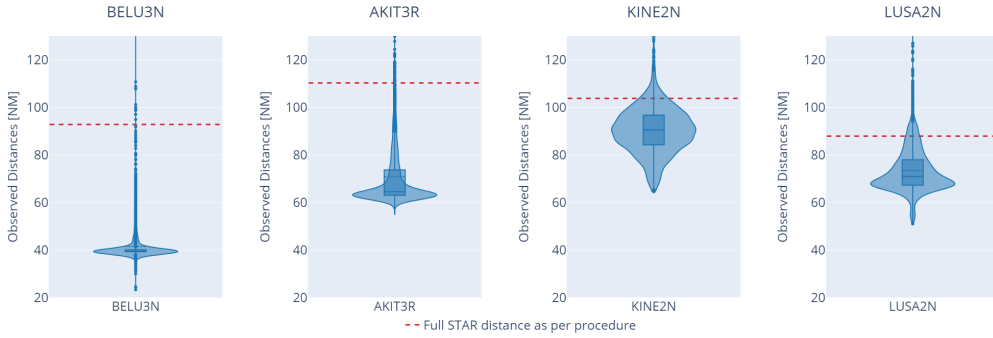


Figure 6. Violin plots with embedded box plots illustrating the overall distribution of the observed flown distances for the four analysed STARs at Geneva Airport (LSGG). The red dashed line marks the full STAR distance according to the published procedure.

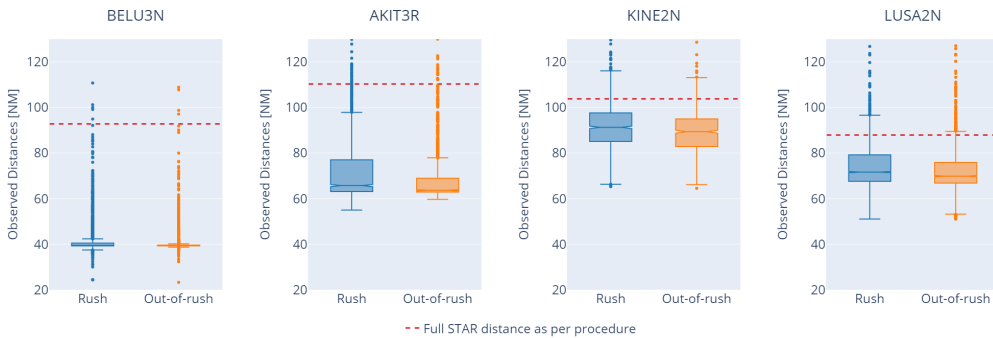


Figure 7. Box plots comparing the distribution of observed flight distances for the four STARs analysed at Geneva Airport (LSGG), separated by rush and out-of-rush periods. The blue boxes represent rush periods, while the orange boxes represent out-of-rush periods. The red dashed line marks the full STAR distance according to the published procedure.

observed distances for *NAPSA 1B*, the 94th percentile for *LANDU 1B*, the 91st percentile for *ROKIL 1A*, and the 95th percentile for *BETOS 1A*.

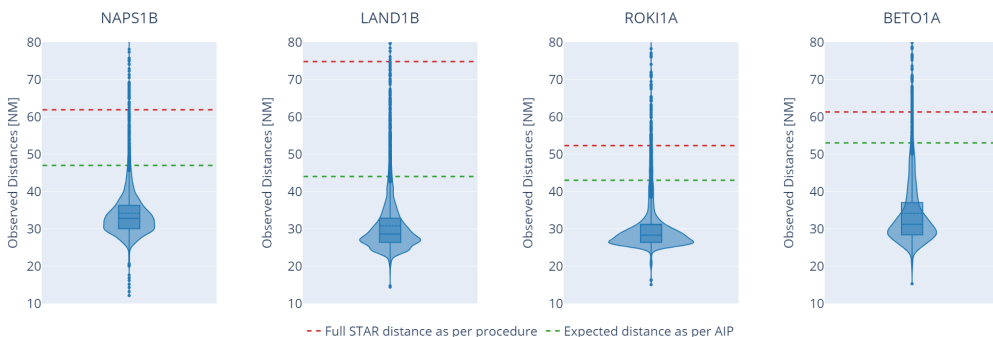


Figure 8. Violin plots with embedded box plots illustrating the overall distribution of observed flown distances for the four analysed STARs at Munich Airport (EDDM). The red dashed line marks the full STAR distance according to the published procedure, while the green dotted line indicates the expected STAR distance as published in the AIP.

The distributions for rush and out-of-rush periods at Munich Airport, shown in Figure 9, again indicate that average flown distances are slightly longer during rush periods for all four STARs. A notable observation from these plots is that the expected STAR distances remain above the range of the box plots, even for the rush hour period. This is, of course, also true for the off-peak periods, where the gap between the expected distance and the upper whisker (1.5 x Interquartile range) is even greater.

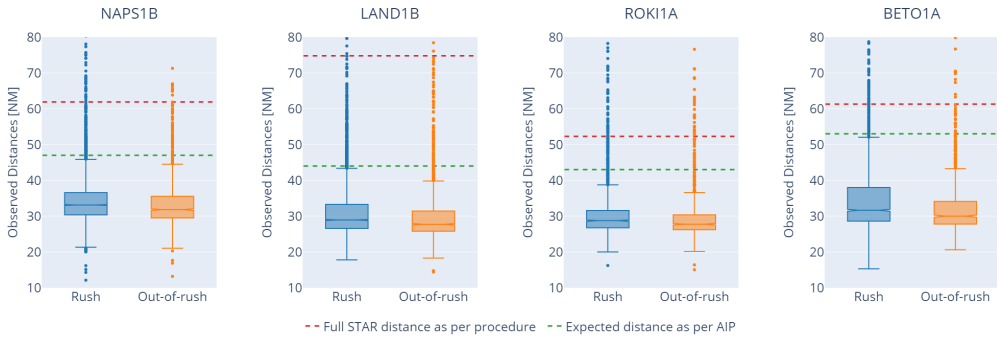


Figure 9. Box plots comparing the distribution of observed flight distances for the four analyzed STARs at Munich Airport (EDDM), conditionally on rush and off-peak periods. The blue boxes represent rush periods, while the orange boxes represent off-peak periods. The red dashed line marks the full STAR distance according to the published procedure, while the green dotted line indicates the expected STAR distance as published in the AIP.

3.3 Rome

As illustrated in Figure 10, most of the flown distances for Rome Airport remain well below the total STAR distance, with only a few outliers matching or exceeding it. Similar to Munich, Rome also has published expected distances, but these only apply to off-peak periods, while the full STAR distance serves as the expected value during peak periods. In contrast to Munich, the expected distance is positioned slightly further within the overall distribution.

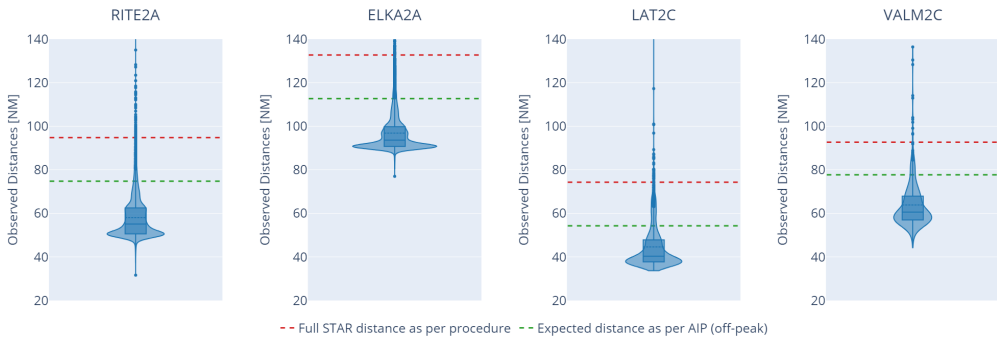


Figure 10. Violin plots with embedded box plots illustrating the overall distribution of observed flight distances for the four STARs analysed at Rome Fiumicino Airport (LIRF). The red dashed line marks the full STAR distance according to the published procedure, while the green dotted line indicates the expected STAR distance as published in the AIP, valid only for off-peak periods.

Analysing the distributions separated by rush and out-of-rush periods, shown in Figure 11, provides more meaningful insights. It becomes clear that during out-of-rush periods, where the expected distance applies, the distributions of observed distances have slightly lower medians. But most im-

portantly, the flight distances are more densely concentrated around shorter distances. It indicates that the majority of aircraft consistently fly shorter routes, and only very few of them fly distances comparable to the nominal STAR distance. Considering only the data from the out-of-rush periods for which they are valid, the expected distances align with the 94th percentile of observed distances for *RITEB 2A*, the 93rd percentile for *ELKAP 2A*, the 85th percentile for *LAT 2C*, and the 90th percentile for *VALMA 2C*.

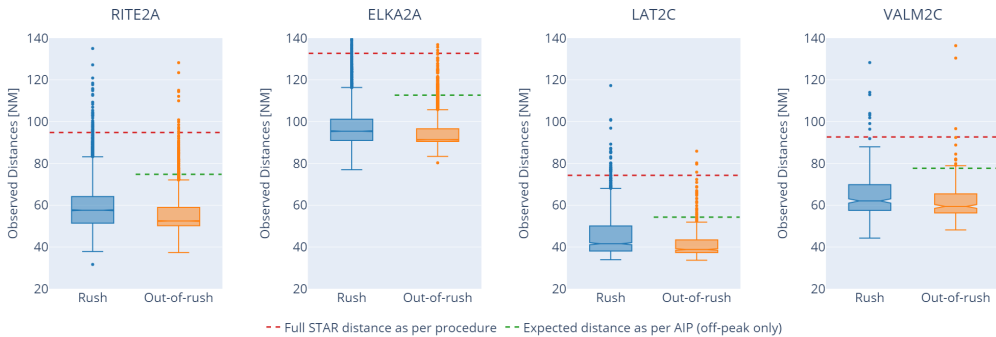


Figure 11. Box plots comparing the distribution of observed flight distances for the four analyzed STARs at Rome Fiumicino Airport (LIRF), separated by rush and off-peak periods. The blue boxes represent rush periods, while the orange boxes represent off-peak periods. The red dashed line marks the full STAR distance according to the published procedure, while the green dotted line indicates the expected STAR distance as published in the AIP, valid only for off-peak periods.

4. Identification of Factors Influencing Flown STAR Distances

Section 3 revealed that significant deviations may occur between the expected and actual flight distances for the selected STARs, particularly when the potential for shortcuts is great and during out-of-rush periods. This section aims to statistically determine the factors that may influence the actual STAR distance flown by an aircraft.

To achieve this, we conducted a linear regression analysis for each airport under consideration. Using the same model structure for all the airports, we focused on the same four STARs per airport that were previously selected. We approach this modeling from an econometric perspective, with the primary goal of understanding how each factor influences flight distance, rather than emphasizing the predictive accuracy of the model. The focus is on interpreting the significance and impact of the variables, providing insights into the underlying relationships rather than solely on forecasting performance.

To ensure consistency and allow for comparison across different STARs at the same airport, we used the ratio of the actual distance flown by an aircraft to the nominal distance of the STAR as the target variable. A value of 1 indicates that the aircraft flew exactly the distance specified in the procedure charts for the STAR. A value less than 1 signifies that the aircraft flew a shorter distance than expected, while a value greater than 1 indicates that the aircraft flew a longer distance than the nominal STAR distance.

All three linear regressions utilize the same set of covariates selected from the dataset described in Section 2. We focused on landing observations corresponding to aircraft types that perform more than 400 landings annually at each respective airport, which together account for over 80% of the total traffic at all three airports. The dataset was further enriched with publicly available features, which are detailed in Table 2.

Table 2. Features used in the regression model, per airport, to predict the ratio between the distance flown and the nominal distance of the STAR.

Feature	Type	Description
STAR	categorical	Name of the STAR flown by the aircraft. Reference: <i>AKIT3R</i> (LSGG); <i>BETO1A</i> (EDDM); <i>ELKA2A</i> (LIRF).
WEEKDAY	categorical	Weekday of the flight. Reference: Monday.
SEASON	categorical	Season of the flight. Reference: Fall.
BODY TYPE	categorical	Body type of the aircraft (either Narrowbody, Widebody, Regional jet, Business jet). Reference: Narrowbody.
RUSH HOUR	boolean	Indicating if the flight landed during rush hours at the considered airport.
Visibility	continuous	Average visibility indicated by the METAR during the approach in km.
Wind speed	continuous	Average wind speed indicated by the METAR during the approach in kts.
Pressure	continuous	Average deviation from standard pressure (1013 hPa) indicated by the METAR during the approach in hPa.
Temperature	continuous	Average temperature indicated by the METAR during the approach in °C.

Figure 12 presents the estimated coefficient for each covariate using the ordinary least squares method for Geneva, Munich and Rome airports respectively. Coefficients shown in red are not statistically different from zero at the 5% level, while those marked with (**) are significant at the 5% level, and (***) at the 1% level.

4.1 Geneva

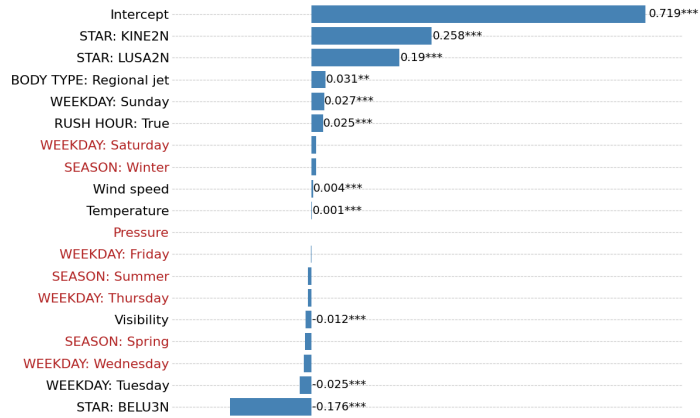
The first linear regression was conducted on 13,706 landing observations at Geneva Airport for the STARs *AKIT3R*, *BELU3N*, *KINE2N*, and *LUSA2N*. The results are shown in Figure 12a. The adjusted R-squared value is 0.329, indicating that the selected covariates only explain a part of the variation in flight distance.

Firstly, the STAR flown significantly impacts the distance ratio. Specifically, under similar conditions, *BELU3N* shows an average distance ratio that is 18% lower compared to *AKIT3R* (the reference group), while *KINE2N* and *LUSA2N* exhibit ratios that are 26% and 19% higher, respectively.

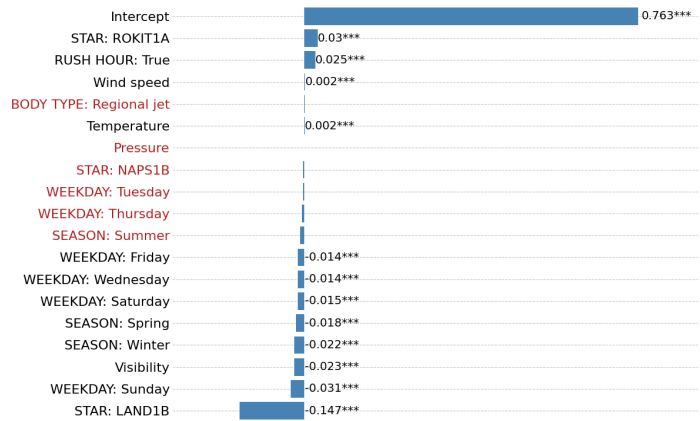
Interestingly, there are statistically significant differences in the distance flown between out-of-rush and rush hours. When all other factors are held constant, aircraft landing during rush hours experience an increase of 2.5% in the distance ratio compared to those landing during out-of-rush hours. The day of the week also appears to affect the distance ratio. For example, the ratio increases by 2.7% on Sunday compared to Monday, while it is 2.5% lower on Tuesday. Ratios for Wednesday, Friday, and Saturday, however, do not differ significantly from Monday's. Seasonal variations seem to have no impact on the distance ratio, as none of the season markers are significantly different from zero.

For the selected STARs, only narrowbody aircraft and regional jets frequently land at Geneva. It seems that under the same conditions, regional jets show an average increase of 3.1% in the distance ratio compared to narrowbody aircraft.

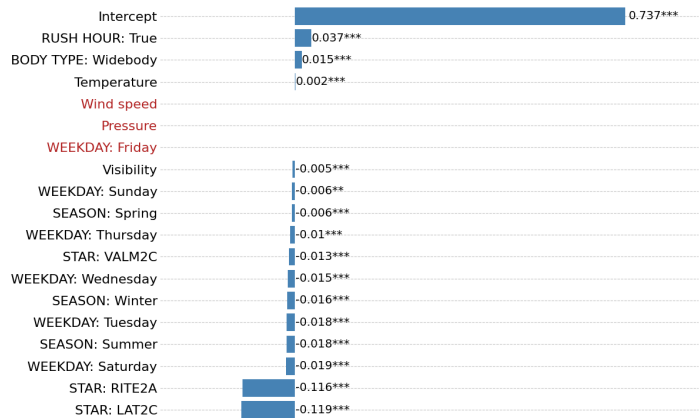
Finally, certain weather parameters have a statistically significant effect on the distance flown. The distance ratio increases by 0.4% for each additional knot of wind speed and by 0.01% for each additional degree Celsius. Although these effects are small, they still statistically contribute to an increase in flight distance. In contrast, visibility has a more pronounced negative impact, with each additional kilometer reducing the distance ratio by 1.2%. Notably, pressure does not have a significant effect on the distance flown.



(a) Coefficient estimates for LSGG.



(b) Coefficient estimates for EDDM.



(c) Coefficient estimates for LIRF.

Figure 12. Results for all three linear regressions indicating the influence of each feature on the ratio between the actual flight distance and the expected STAR distance. Features in red are not significantly different from zero, whereas (**) indicates a 5% confidence level, and (***) a 1% confidence level.

4.2 Munich

The second linear regression analysis is based on 17,526 landings at Munich Airport for the STARS *BETO1A*, *LAND1B*, *NAPS1B*, and *ROKI1A*. The results, illustrated in Figure 12b, show an adjusted R-squared value of 0.155, suggesting that the selected covariates may not fully explain the variations in the distance ratio. However, the linear regression still provides valuable insights from an econometrical point of view.

At Munich, the variations across STARS are less pronounced compared to Geneva. The reference group, *BETO1A*, and *NAPS1B* are not significantly different in terms of the distance ratio, while *ROKI1A* shows only a 3% increase in the distance ratio. In contrast, *LAND1B* exhibits a significantly shorter flown distance, with an average distance ratio 14% lower than that of *BETO1A*.

Similar to the results from Geneva, the distance ratios in Munich are significantly affected by rush hours. Under equal conditions, landings during rush hours show a 3% increase in the distance ratio. The day of the week also plays a role, with Wednesday, Friday, and Saturday associated with approximately a 2% decrease in the distance ratio and Sunday showing a 3% decrease. Tuesday and Thursday do not differ significantly from Monday. Regarding seasonal effects, winter and spring show a 2% decrease in the distance ratio compared to fall, while summer is comparable to fall. Widebody and business jets are not represented in the selected STARS for Munich. Moreover, there are no statistically significant differences in the distance ratio between narrowbody aircraft and regional jets.

Finally, weather parameters also influence the distance ratio. Wind speed and temperature both result in a 0.2% increase in the distance ratio for each additional unit, while visibility has a notable negative effect. For every additional kilometer of visibility, the distance ratio decreases by over 2%.

4.3 Rome

The final linear regression analysis covers 20,337 observations for the STARS *ELKA2A*, *LAT2C*, *RITE2A*, and *VALM2C*. The results are displayed in Figure 12c, with an adjusted R-squared value of 0.261, indicating a moderate model fit.

Compared to the reference STAR *ELKA2A*, *VALM2C* shows a 1.3% lower distance ratio, while *LAT2C* and *RITE2A* have significantly lower ratios, approximately 11% less than *ELKA2A*.

As observed at the other airports, rush hours also have a statistically significant effect on the distance ratio and this effect is even more pronounced in Rome. During rush hours, the distance ratio increases by just under 4%. The day of the week also influences the distance ratio: Monday and Friday have the highest ratios, while Sunday, Thursday, and Wednesday show reductions of around 1%. Saturday sees the most significant reductions, with a 2% lower distance ratio, suggesting more shortcuts. Interestingly, all seasons show statistically significant differences in the distance ratio. Fall exhibits the highest distance ratio, while winter and summer have the lowest, with reductions of nearly 2%.

The dataset for Rome airport does not include business jets or regional jets. Widebody aircraft tend to have longer STAR distances than narrowbody aircraft, with an average increase of 1.5% in the distance ratio.

Finally, meteorological parameters seem to have a much smaller influence in Rome compared to the other airports. Temperature slightly increases the distance ratio, and visibility decreases it by only 0.5%. Pressure and wind speed do not appear to have any significant effect on the ratio.

5. Fuel Saving Potential

The analysis in Section 3 has shown significant discrepancies between the full STAR distance and the distances flown, which are mitigated by the publication of expected distances. To estimate the potential fuel savings from the introduction of expected distances for STARs that currently lack this information, a sample calculation was performed. The *BELUS 3N* approach at Geneva was selected for this analysis as it has a particularly large discrepancy between the full STAR distance and the distances actually flown, resulting in a large savings potential.

For this analysis, a fictional flight of an Airbus A220-300 from Porto (LPPR) to Geneva (LSGG) on 10.10.2024 was used, which was assumed to use the *BELUS 3N* approach into Geneva. The Porto-Geneva route was chosen because its flight time is about two hours, which aligns with the average short-haul flight to Geneva operated by Swiss International Air Lines. Using CAE’s Flight Plan Manager v6.5.1 software, three versions of an Operational Flight Plan (OFF), each detailing the required fuel amounts for different scenarios, were generated for this flight. Extracts from these plans are presented in Figure 13.

LX9001	10Oct24Z	OPO/GVA	RLS 1 / 1
LW9001	LPPR/OPO	13.00z (13.00z)	
HB-JCAZ	LSGG/GVA	15.30z (15.10z)	
BCS3		02.30 (02.10)	
Remarks			
MEL/CDL: ITEMS AFFECTING OFF NOT CONSIDERED			
Route ID: Z1 BELUS3N STAR			
DIST 849 GCI 120 CP T46			
MIN TEMP M56 @ (N4424.9 E00245.7) MAX SHR			
Speed: CI19			
Steps: F360 ZMR/F380 MEN/F300			
N4114.1 W00840.7	Departure ATIS		
227ft			
FL360/M52/48495			
Wind 258/057			
ZFW 50000	ATC Departure Cle		
TOF 6149			
TOW 56149			
TRIP 3667	Arrival ATIS		
LW 52482			
REMF 2482			
REMT 1.32			
BASIC			
TAXI 90 .10			
TRIP 3667 1.55			
CONT5% 184 .06			
ALTN LFLL 990 .31			
ADD			
EXTRA 537 .20			
FINAL RES 771 .30			
MIN BLOCK 6239 3.22			
DISCF			
BLOCK			

LX9001	10Oct24Z	OPO/GVA	RLS 2 / 1
LW9001	LPPR/OPO	13.00z (13.00z)	
HB-JCAZ	LSGG/GVA	15.30z (15.02z)	
BCS3		02.30 (02.02)	
Remarks			
MEL/CDL: ITEMS AFFECTING OFF NOT CONSIDERED			
Route ID: Z2 STRAIGHT IN			
DIST 792 GCI 112 CP T48			
MIN TEMP M56 @ (N4424.9 E00245.7) MAX SHR			
Speed: CI19			
Steps: F360 ZMR/F380 MEN/F300			
N4114.1 W00840.7	Departure ATIS		
227ft			
FL360/M52/48495			
Wind 258/057			
ZFW 50000	ATC Departure Cle		
TOF 6149			
TOW 56149			
TRIP 3423	Arrival ATIS		
LW 52726			
REMF 2726			
REMT 1.41			
BASIC			
TAXI 90 .10			
TRIP 3423 1.47			
CONT5% 172 .05			
ALTN LFLL 991 .31			
ADD			
EXTRA 537 .20			
FINAL RES 771 .30			
MIN BLOCK 5447 2.53			
DISCF			
BLOCK			

LX9001	10Oct24Z	OPO/GVA	RLS 3 / 1
LW9001	LPPR/OPO	13.00z (13.00z)	
HB-JCAZ	LSGG/GVA	15.30z (15.02z)	
BCS3		02.30 (02.02)	
Remarks			
MEL/CDL: ITEMS AFFECTING OFF NOT CONSIDERED			
Route ID: Z2 STRAIGHT IN			
DIST 792 GCI 112 CP T48			
MIN TEMP M56 @ (N4424.9 E00245.7) MAX SHR			
Speed: CI19			
Steps: F360 ZMR/F380 MEN/F300			
N4114.1 W00840.7	Departure ATIS		
227ft			
FL360/M52/48495			
Wind 258/057			
ZFW 50000	ATC Departure Cle		
TOF 5883			
TOW 55883			
TRIP 3413	Arrival ATIS		
LW 52470			
REMF 2470			
REMT 1.32			
BASIC			
TAXI 90 .10			
TRIP 3413 1.47			
CONT5% 171 .05			
ALTN LFLL 991 .31			
ADD			
EXTRA 537 .20			
FINAL RES 771 .30			
MIN BLOCK 5973 3.13			
DISCF			
BLOCK			

(a) Scenario 1: OPO-GVA flight, carrying the fuel required for the full BELUS 3N STAR procedure and following the full STAR route.

(b) Scenario 2: OPO-GVA flight, carrying the fuel required for the full BELUS 3N STAR procedure but flying a straight-in approach.

(c) Scenario 3: OPO-GVA flight, carrying the fuel required for a straight-in approach and flying a straight-in approach.

Figure 13. Operational flight plans for a fictional OPO-GVA flight illustrating three different scenarios. The red box highlights the trip fuel required for each of the scenarios.

For each of the three OFFs, a consistent aircraft mass, the usual route for that city-pair and the specific meteorological conditions for that day were used. Each flight plan also includes the same allocations of taxi fuel, alternate fuel for diversion to Lyon (LFLL), 5% contingency fuel and 20 minutes of discretionary fuel to cover scenarios such as a weather-related second approach or holding

at the destination.

The differences between the three OFPs lie in the amount of fuel carried for the STAR procedure and the actual STAR route flown. The first OFP, shown in Figure 13a, represents a flight carrying fuel for the full *BELUS 3N* STAR procedure and flying the full procedure, resulting in a trip fuel requirement of 3667 kg. The second OFP, shown in Figure 13b, represents a flight performing a straight-in approach to Geneva via BELUS, CBY and INDIS (see Figure 1b) with additional discretionary fuel added to match the total fuel load of the previous OFP. This scenario simulates a flight executing a straight-in approach but carrying fuel for the full *BELUS 3N* STAR, requiring 3423 kg of trip fuel. The third and final OFP in Figure 13c reflects a flight also performing a straight-in approach, but carrying only the fuel required for such a direct approach, resulting in a reduced trip fuel requirement of 3413 kg.

The difference of 254 kg of trip fuel between the first and third scenarios corresponds to the additional fuel required to fly the full STAR compared to a straight-in approach when carrying only the required amounts of fuel for both scenarios. Meanwhile, the 10kg difference between the second and third OFPs reflects the fuel used to carry the additional 254kg required for the full STAR procedure, which is not flown. Thus, for a standard two-hour short-haul flight using the *BELUS 3N* STAR, approximately this amount of fuel could be saved by providing expected distances that more closely match actual flown distances for fuel planning.

Due to a simpler implementation in the flight planning software, the fuel calculation for the straight-in approach is based on a direct route via BELUS, CBY and INDIS, rather than an expected distance derived from a specific percentile of observed distances. This value indicates the maximum potential fuel savings that could be achieved if a short straight-in STAR were published and planned. A more conservative approach, such as using the 90th percentile of observed STAR distances, would increase the distance by about 3 NM.

It should also be mentioned that in addition to using the expected distances published in the AIP, operators have other options that provide some flexibility to adapt fuel planning to better reflect reality. Annex IV, Part CAT of Regulation (EU) No 965/2012[9] also covers exceptions beyond the published expected STAR distances, including point merge and trombone-type STAR procedures. For these arrivals, operators may always consider the direct distance to the merge point or the expected routing for the calculation of the trip fuel, while any additional fuel required to fly a longer procedure will be covered by contingency fuel. For such procedures it is also common for expected distances to be published to aid operators with fuel planning. In addition, three fuel planning schemes were introduced into the regulations in 2022 to allow operators to better tailor fuel planning to their operational needs: *basic scheme*, *basic scheme with variations*, and *individual scheme*. The basic scheme with variations allows the contingency fuel to be adjusted using methods such as Statistical Contingency Fuel (SCF). This method adjusts the contingency fuel based on historical data rather than using a fixed percentage of the trip fuel. The individual scheme goes even further, allowing operators to customise the entire fuel planning process based on their own operational data and risk assessments.

6. Discussions

Analysis of the actual distances flown has shown that there are significant differences between the full star distance and the observed distances for all STARs at Munich and Rome, and for two STARs at Geneva Airport. However, for Munich and Rome, the published expected STAR distances correct for this and are much closer to the observed distances. In fact, the results suggest that the expected distances for Munich were defined by using the overall distribution of historical distances flown and setting the expected distance somewhere around its 90th to 95th percentile. A similar approach

appears to have been used for Rome, but only data for the out-of-rush period is used. Overall, the published distances for both airports reduce the discrepancy between the distances used for fuel planning and the actual distances flown while still covering the majority of flights.

The analysis of factors influencing the flown distance has shown that there are notable differences between STARS in terms of distance reduction potential, which largely depends on their shapes and opportunities for shortcuts. For example, the *BELU3N* STAR at Geneva Airport offers substantial shortcut potential, with average flights covering only half of its nominal distance. In contrast, the simpler-shaped *KINE2N* STAR, which has low shortcut potential, results in flights covering 98% of its nominal distance. As anticipated, the time of the day significantly affects its flight distance, with rush-hour landings increasing distances at all three airports, especially in Rome, which adjusts its expected approach distance based on rush vs. out-of-rush hours. However, even during rush hours, when the full STAR distance is suggested for the calculation of fuel, the average observed flight distance at Rome is only 78% of the full STAR distance. Seasons and days of the week appear to affect approach distances differently at different airports, probably due to variations in tourist traffic or local weather conditions. Meteorological conditions, however, appear to have a consistent effect on approach distance regardless of location. An increased visibility decreases the flight distance, whereas higher temperatures, pressures, and wind speeds tend to slightly increase it.

The results on the fuel-saving potential indicate that the introduction of expected STAR distances for the *BELUS 3N* STAR in Geneva would result in a saving of approximately 10 kg of fuel for a standard short-haul flight of around 2 hours flight duration that uses this arrival route. While this might seem modest on a per-flight basis, the cumulative effect over many flights quickly leads to significant amounts of fuel that could be saved. For example, in the hypothetical scenario where two daily Porto-Geneva flights operated by an Airbus A220-300 were to exclusively use the *BELUS 3N* STAR to Runway 04 for an entire year, the total fuel savings would amount to approximately 7,300 kg. When summed up for all yearly flights using the *BELUS 3N* approach, or even across a wide range of STARS at various airports, the amount of fuel saved through the publication of expected STAR distances becomes relevant. The 10kg saving demonstrated for the A220 flight is a conservative estimate compared to potential savings on other flights. For larger aircraft and longer routes, the fuel savings would be even greater as the cost of carrying extra fuel increases with flight distance.

Although there are alternative fuel planning adjustments that could potentially be used to mitigate the impact of STAR shortcuts, they have clear disadvantages compared to publishing expected STAR distances. For example, while SCF can reduce the impact of such shortcuts, its calculations are based generally based on historical data for specific city-pair and aircraft-type combinations. This may include a range of approaches and runways, as well as other en-route factors, meaning that a specific STAR discrepancy may not be fully compensated. In addition, SCF only allows for adjustments of the contingency fuel. In the example fuel calculation for the *BELUS 3N* approach, the reduction in carried trip fuel when using the straight-in approach exceeds the contingency fuel being carried, making SCF insufficient to fully compensate for the discrepancy. On the other hand, the use of the individual fuel scheme could more effectively correct systematic STAR shortcuts. However, this approach requires advanced fuel management systems, sophisticated planning tools, operational data analysis, and robust safety performance management. As a result, it is generally only a viable option for large operators with such systems in place.

While the primary objective of publishing expected STAR distances is to improve fuel planning, this information also provides benefits in other areas. Having the information about expected track miles helps pilots to manage in-flight descent planning, especially at unfamiliar or infrequently visited airports. This factor is especially significant for continuous descent operations, as accurate STAR distance estimates can greatly enhance the determination of the top of descent point. In addition,

considering expected STAR distances in the flight planning phase could potentially help operators predict arrival times more accurately, allowing better coordination for turnarounds.

7. Conclusion

This study highlights the positive impact of publishing expected STAR distances on improving fuel efficiency. By analysing ADS-B data from Geneva, Munich, and Rome airports, it has been shown that the expected STAR distances published in the AIPs for Munich and Rome more closely match the actually flown distances compared to the full procedure distances. These expected distances, which can be used in pre-flight fuel planning, help reduce the discrepancies between full and flown distances observed for various STARs at all three airports. The subsequent modelling approach, developed to further investigate the factors affecting flown distances, identified key influences such as STAR design, rush hour traffic, and weather conditions. A sample fuel calculation for the *BELUS 3N* approach at Geneva also showed that implementing expected distances for this approach would result in savings of around 10kg of fuel on a standard short-haul flight using this approach.

Overall, the results suggest that extending the publication of expected STAR distances to more airports with systematic deviations between full and flown STAR distances would be an easily implemented solution to improve fuel efficiency and promote environmental sustainability. Unlike other fuel optimization methods such as SCF, the publication of expected STAR distances specifically addresses deviations from published procedures for STARs without requiring complex management systems from operators, making it a practical and beneficial solution for all operators. Given the limited prior research on this topic, this study fills a critical gap by illustrating the benefits of publishing expected STAR distances. It also raises awareness of this little-known topic and encourages further research and discussion. Future research could extend the analysis to a wider range of airports and STARs, providing a clearer understanding of the prevalence of the problem and a more comprehensive assessment of the potential fuel savings that could be achieved through wider implementation.

Author Contributions

- Jan Krummen: Conceptualization, Data Curation, Formal analysis, Methodology, Software, Writing – original draft, Writing – review & editing
- Timothé Krauth: Conceptualization, Data Curation, Formal analysis, Methodology, Software, Writing – original draft, Writing – review & editing
- Jan Allendorf: Conceptualization, Data Curation, Formal analysis, Writing – review & editing
- Raphael Monstein: Conceptualization, Writing – review & editing

Funding Statement

No funding was received for this research.

Open Data Statement

All the data that is required for the reproduction of the presented results is available on under <https://zenodo.org/records/13869475>.

Reproducibility Statement

The code required to reproduce all results presented in this paper can be found in a public GitHub repository under the following link: https://github.com/ZHAW-ZAV/STAR_shortcut_OSN_paper. The only exception in terms of reproducibility relates to the calculation of fuel savings, as this was carried out using licensed flight planning software, which imposes certain limitations on the reproducibility of this part.

References

- [1] *Annex 6 to the Convention on International Civil Aviation: Operation of Aircraft*. 12th edition. Montreal, Canada, 2022.
- [2] Flight Standards Service U.S. Department of Transportation Federal Aviation Administration. *Instrument Procedures Handbook*. 2017.
- [3] International Civil Aviation Organization. *Doc9976 - Flight Planning and Fuel Management (FPFM)*. Montreal, Canada: International Civil Aviation Organization (ICAO), 2015.
- [4] Deutsche Flugsicherung GmbH (DFS). *AIP IFR Deutschland*. Accessed: 2024-08-26. 2024. URL: <https://aip.dfs.de/basicAIP/>.
- [5] Ente Nazionale Assistenza al Volo (ENAV). *ITALY Aeronautical Information Publication (AIP)*. Accessed: 2024-08-26. 2024. URL: [https://onlineservices.enav.it/enavWebPortalStatic/AIP/AIP/\(A08-24\)_2024_08_08/index.html](https://onlineservices.enav.it/enavWebPortalStatic/AIP/AIP/(A08-24)_2024_08_08/index.html).
- [6] Matthias Schäfer, Martin Strohmeier, Vincent Lenders, Ivan Martinovic, and Matthias Wilhelm. “Bringing up OpenSky: A large-scale ADS-B sensor network for research”. In: *IPSN-14 Proceedings of the 13th International Symposium on Information Processing in Sensor Networks*. IEEE. 2014, pp. 83–94.
- [7] Xavier Olive. “traffic, a toolbox for processing and analysing air traffic data”. In: *Journal of Open Source Software* 4 (2019), p. 1518. ISSN: 2475-9066. DOI: 10.21105/joss.01518.
- [8] EUROCONTROL. *AIU Airport Performance Dashboard*. <https://ansperformance.eu/dashboard/stakeholder/airport/db/>. (Accessed on 2024-09-27).
- [9] European Union Aviation Safety Agency (EASA). *Annex IV to Regulation (EU) No 965/2012: Air Operations - Commercial Air Transport (CAT) Operations, Revision 21*. <https://www.easa.europa.eu/document-library/regulations/annex-iv-regulation-eu-no-9652012>. Accessed: 2024-10-01. 2023.